ChemComm

COMMUNICATION

View Article Online
View Journal | View Issue

Cite this: *Chem. Commun.*, 2023, 59, 5451

Received 27th January 2023,
Accepted 6th April 2023

DOI: 10.1039/d3cc00374d

rsc.li/chemcomm

HF-Free synthesis of colloidal Cs_2ZrF_6 and $(NH_4)_2ZrF_6$ nanocrystals†

Eden Tzanetopoulos, Julie Schwartz and Daniel R. Gamelin *

A solution-phase synthesis of colloidally stable A_2BF_6 nanocrystals is reported for the first time, focusing on $A^+ = Cs^+$, NH_4^+ and $B^{4+} = Zr^{4+}$. Handling hypertoxic HF is avoided by using NH_4F and a low-boiling-point alcohol, representing the first synthesis of any A_2BF_6 nanocrystals without HF addition. The chemical incompatability of Zr^{4+} with other common fluoride sources is discussed.

Colloidal fluoride nanocrystals (NCs) of lattices involving trivalent cations, such as $NaYF_4$, LaF_3, and $LiLuF_4$, have been extensively studied for uses in bioimaging, optoelectronics, X-ray scintillation, laser cooling, optical thermometry, anticounterfeiting, and lighting, among others.[1–3] These lattices offer high optical transparency and chemical stability, and their optical functionality can be tailored *via* facile doping with trivalent lanthanide ions.[4] They provide reasonably low phonon energies that favour high lanthanide photoluminescence quantum yields (PLQYs). Isovalent substitution by trivalent lanthanides also supports site homogeneity, narrow emission lines, and low trap densities. Fluoride NCs based on divalent (*e.g.*, SrF_2, FeF_2, MnF_2) and monovalent (*e.g.*, NaF, LiF) cations have also been widely investigated.[5–8] Despite the tremendous popularity of colloidal fluoride NCs, however, those involving tetravalent cations (such as A_2BF_6, $A^+ = K^+$, Na^+, Cs^+; $B^{4+} = Zr^{4+}$, Si^{4+}, Ti^{4+}, Ge^{4+}, Sn^{4+}) remain almost completely unexplored. In bulk, A_2BF_6 lattices doped with Mn^{4+} ions are leading candidates for narrow-line red emitters in display and lighting technologies,[9,10] and those doped with Re^{4+} show efficient upconversion.[11] The host A- and B-site cations also affect the B-site's local symmetry, which allows fine-tuning of dopant spectral linewidths, peak positions, and lifetimes.[12,13] Access to these materials as colloidal NCs could reduce light scattering in conventional optoelectronics applications, facilitate surface functionalization, and enable entirely unprecedented opportunities in solution-phase processing, such as electrohydrodynamic ink-jet printing.[14,15] Here, we report the first hot-injection synthesis of colloidally stable A_2BF_6 NCs, Cs_2ZrF_6 and $(NH_4)_2ZrF_6$.

Hydrofluoric acid (HF) has been inextricably linked to the syntheses of A_2BF_6 crystals for decades.[16–18] Although a very effective fluoride source, the inherent chemical and environmental hazards of handling HF, and the accompanying safety-engineering costs, make syntheses requiring HF handling difficult to justify or scale up and potentially hinder commercialization of many promising fluoride materials. Consequently, there is growing interest in development of A_2BF_6 syntheses that do not require addition of HF. Polycrystalline A_2BF_6 powders have now been successfully prepared without this precursor,[19,20] but colloidal NCs have not. Until very recently, in fact, there were no reports of any type of colloidal A_2BF_6 NCs, made with or without addition of HF. The sole report[21] of colloidal A_2BF_6 NCs to date describes the syntheses of Cs_2SnF_6, Cs_2SiF_6, and K_2SiF_6 NCs *via* a co-precipitation method in which crystalline powders of the pre-formed fluoride lattices were dissolved in concentrated HF (40%, aqueous) and injected into solutions of organic ligands in polar solvent at room temperature. Mn^{4+} doping was achieved by co-dissolution of bulk A_2MnF_6 in the HF solution. The use of HF is undesirable for health and environmental reasons, and there is a need for alternative syntheses.

Recent works have successfully prepared mixed-metal fluoride bulk powders of A_2MnF_4 ($A^+ = K^+$, Rb^+, Cs^+) and $RbMF_3$ ($M^{2+} = Mg^{2+}$, Ca^{2+}) using metal-trifluoroacetates ($M(tfa)_n$) as a safer single-source fluoride precursor *via* both solid-state and solution-phase syntheses.[22,23] Trifluoroacetic acid (TFA) has also been used as a fluoride source in preparing a variety of colloidal NCs (*e.g.*, $NaYF_4$, LaF_3, FeF_3).[5,24,25] TFA (or tfa) does not liberate F^- until its decomposition between 250 and 300 °C, creating a controlled and tuneable release of reactive F^- ions into solution. We therefore attempted to adapt an attractive solution-phase synthesis[24] of $NaYF_4$ NCs using TFA for the synthesis of Cs_2ZrF_6 NCs. Our attempts did not yield any discernible crystalline fluoride products (Fig. S1, ESI†). Further investigation suggested that TFA is chemically incompatible with the oxophilic tetravalent

Department of Chemistry, University of Washington, Seattle, Washington, 98195-1700, USA. E-mail: gamelin@uw.edu

† Electronic supplementary information (ESI) available: Complete experimental details and additional TEM and XRD data. See DOI: https://doi.org/10.1039/d3cc00374d

B-site cations at the elevated temperatures necessary to release F^- under our conditions. Indeed, related attempts to prepare bulk metal-fluorides by calcination of TFA complexes of various cations (*e.g.*, Li^+, Na^+, Pb^{2+}, Y^{3+}, Ti^{4+}, Zr^{4+}) yielded the desired fluoride salts in every case except the two 4+ cations (Zr^{4+} and Ti^{4+}), which instead yielded metal-oxyfluoride products.[26] Release of gaseous oxygen-based byproducts during decomposition of $M(tfa)_n$ precursors at $T \geq 300$ °C has been observed in syntheses of mono-, di-, and trivalent metal-fluorides,[27,28] and such species may interfere with formation of the target Cs_2ZrF_6 lattice by binding to the highly oxophilic B^{4+} ions. Alternatively, we do note a promising recent demonstration that solid-state thermolysis of the alkali trifluoroacetates $KH(tfa)_2$ and $CsH(tfa)_2$ will fluorinate a-SiO_2 to form crystalline K_2SiF_6 and Cs_2SiF_6,[29] albeit under conditions very different from those required to form colloidal NCs.

The unsuitability of TFA as a F^- precursor for A_2BF_6 NC synthesis led us to consider alternative fluoride sources that offer greater reactivity at lower temperatures. Anhydrous fluoride salts such as tetramethylammonium fluoride have been shown to replace the chloride and tosylate groups of organic complexes in polar solvents at room temperature,[30] and we hypothesized that these may also circumvent the B^{4+}-oxo impasse encountered with TFA. Critically, handling these solids rather than liquid HF vastly reduces the risk of accident and is thus highly advantageous from a safety standpoint. We decided to investigate NH_4F as a fluoride source for the synthesis of A_2BF_6 NCs.

Solvent polarizability has a prodigious impact on the reactivity of ammonium-based fluoride salts.[31] Non-polar solvents cause the formation of low-reactivity salt aggregates, whereas polar solvents favour free fluoride ions. We therefore decided to explore the addition of NH_4F and methanol (MeOH) to generate active F^- ions in non-polar solutions of Zr-oleate. The high volatility of MeOH ensures that it can be swiftly pulled off under vacuum after mixing, without further chemical consequence. NH_4F in MeOH has been used in solution-phase syntheses of other fluoride NCs (*e.g.*, core–shell doped $NaGdF_4$ and Yb,Er/Tm-doped $NaYF_4$), with promising results.[32,33] Most encouragingly, NH_4F in MeOH has also been used to prepare Yb,Er-doped Na_3ZrF_7 NCs, involving the Zr^{4+} cation.[34]

In an initial attempt at preparing Cs_2ZrF_6 NCs, MeOH, NH_4F (solid), and CsOH were added to a room-temperature solution of Zr-oleate in 1-octadecene. MeOH was removed under vacuum, and the remaining solution was heated to and kept at 250 °C for 10 min before cooling (experimental details in ESI†). Fig. 1a shows a transmission electron microscope (TEM) image of the resulting product, revealing microcrystals of various sizes and morphologies. Fig. 1b shows the corresponding powder X-ray diffraction (pXRD) data. The only crystalline product detected is trigonal-phase Cs_2ZrF_6. Poorly controlled nucleation and growth likely causes the wide distribution of crystallite sizes observed in Fig. 1a. Nonetheless, these data demonstrate that NH_4F can be used as a fluoride precursor for the synthesis of Cs_2ZrF_6 under these conditions.

The successful preparation of A_2BF_6 crystallites using NH_4F at 250 °C indicates that this chemistry is not impeded by the same kind of B^{4+}-oxo bond formation encountered with TFA. A major difference between the two fluoride sources is that NH_4F in MeOH offers a high F^- chemical potential already at room temperature, whereas TFA requires high temperatures to liberate any F^- and it likely never generates an equivalent F^- chemical potential under experimentally accessible conditions.

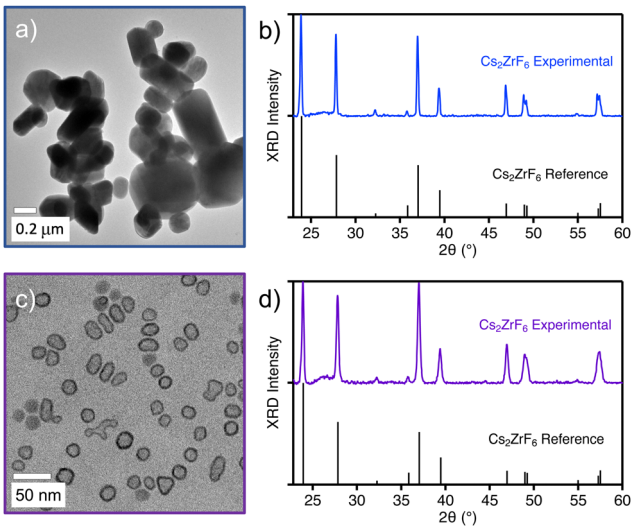

Fig. 1 (a) TEM image and (b) pXRD data of Cs_2ZrF_6 microcrystals *via* one-step-addition synthesis. (c) TEM image and (d) pXRD data of hollow Cs_2ZrF_6 NCs after 10 min reaction time. pXRD data are compared to Cs_2ZrF_6 (trigonal, ICSD Coll. Code 25598) reference.

To better control crystal nucleation, the above synthesis of Cs_2ZrF_6 was restructured to now involve injection of Cs-oleate into a reaction pot containing the Zr^{4+} and F^- precursors, held at 250 °C. Aliquots of the reaction solution were taken at various times between 1 and 55 min (Fig. S2, ESI†). Fig. 1c and d show a TEM image and pXRD data for the 10 min product. The pXRD data again show only trigonal-phase Cs_2ZrF_6, with no detectable crystalline impurities. The TEM image shows that this procedure now yields NCs instead of microcrystals. Scherrer analysis of the pXRD linewidths indicates an estimated lattice coherence length of ~20 nm. Interestingly, the TEM data also show that many of the Cs_2ZrF_6 NCs are hollow, validated by high-angle dark-field scanning TEM (Fig. S12, ESI†).

Hollowing has been observed in a variety of fluoride NCs,[35,36] and in some cases a sensitivity to surfactants has been demonstrated.[37] We thus hypothesized that altering the surface chemistry may affect NC hollowing. Following the same hot-injection procedure described above, capping ligands trioctylphosphine and oleylamine were now introduced to the reaction solution, in addition to oleic acid. Aliquots were collected 1 and 3 min after hot-injection. These additional surfactants did not affect hollowing at either time point (Fig. S3, ESI†). Instead, this synthesis again produced non-uniform hollow NCs. We then looked to alter the reaction temperature. We found that reaction temperatures (T_{rxn}) above 200 °C consistently yielded inhomogeneous and hollow Cs_2ZrF_6 NCs (Fig. S4, ESI†). At T_{rxn} = 180 °C, though, solid Cs_2ZrF_6 NCs were successfully formed. This 180 °C synthesis is summarized in Fig. 2.

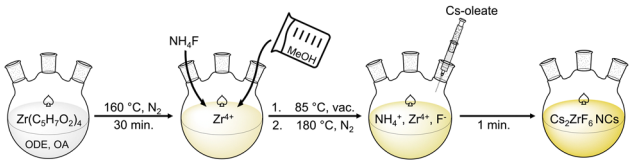

Fig. 2 T_{rxn} = 180 °C Schlenk-line synthesis of colloidal Cs_2ZrF_6 NCs.

Fig. 3a and b shows TEM images of representative Cs_2ZrF_6 NCs prepared by this method, quenched 1 min after hot-injection. These images show hexagonally shaped NCs with a narrow size distribution (d = 26.5 ± 2.0 nm). This result is consistent with the Cs_2ZrF_6 crystalline domain size of ~26 nm estimated using Scherrer analysis of pXRD linewidths. Note that minor holing is observed in the TEM images of some Cs_2ZrF_6 NCs prepared by this route; TEM measurements as a function of electron-beam exposure show that this holing is caused by beam damage during imaging, and that it is therefore clearly distinct from the high-temperature hollowing discussed above (see ESI†). Fig. 3c plots pXRD data of the washed reaction precipitate. These data again show trigonal-phase Cs_2ZrF_6, but now also show a minor impurity identified as cubic CsF. The CsF grain size was estimated to be > ~50 nm from its pXRD linewidths, but TEM reveals that these CsF particles actually aggregate into large clusters (≫100 nm, see ESI† Fig. S8 and discussion for further details). Because of its large size, the CsF impurity is easily separated from the Cs_2ZrF_6 NC solution by simple centrifugation, as confirmed using electron diffractometry of the collected supernatant (Fig. S6, ESI†). Fig. 3d shows a photograph of the final colloidal Cs_2ZrF_6 NCs in hexane solution, highlighting the first colloidal Cs_2ZrF_6 NCs, and the first colloidal A_2BF_6 NCs of any composition prepared without handling HF.

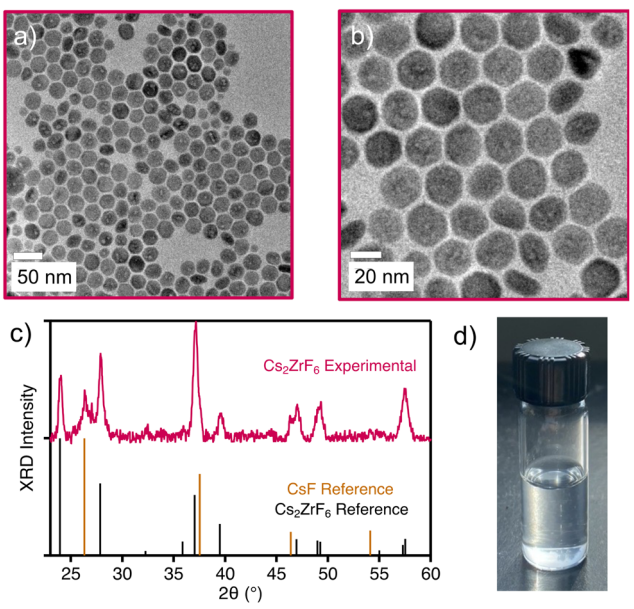

Fig. 3 (a and b) TEM images of Cs_2ZrF_6 NCs. (c) pXRD data of Cs_2ZrF_6 NCs. A minor CsF impurity is observed. For comparison, Cs_2ZrF_6 (trigonal, ICSD Coll. Code 25598) and CsF (cubic, ICSD Coll. Code 61563) references are given. (d) Cs_2ZrF_6 NCs suspended in hexane.

To understand the mechanism by which Cs_2ZrF_6 NCs form, and the hollowing observed at elevated temperatures, aliquots taken from heated reaction mixtures *prior* to Cs-oleate injection were investigated by pXRD and TEM. Remarkably, hexagonal $(NH_4)_2ZrF_6$ NCs were found in these precursor solutions at all temperatures between 180 and 250 °C (Fig. 4 and Fig. S9, ESI†). $(NH_4)_2ZrF_6$ NCs thus form during precursor heating and are already present prior to Cs-oleate injection. Injection of Cs-oleate then converts these NCs into Cs_2ZrF_6 NCs by rapid A-site cation exchange. Whereas cation exchange at 180 °C yields isomorphic hexagonal Cs_2ZrF_6 NCs, the observation of hollow Cs_2ZrF_6 NCs at temperatures above 200 °C suggests faster outward diffusion of NH_4^+ from within the $(NH_4)_2ZrF_6$ lattice than inward diffusion of Cs^+, *i.e.*, a nanoscale Kirkendall effect.[38] These findings are summarized in Fig. 4. The formation of large CsF crystallites as a byproduct at 180 °C is likely caused by the excess Cs^+ and F^- ions in solution prior to cation exchange, but over time this CsF redissolves and contributes to growth of the Cs_2ZrF_6 NCs (Fig. S5, ESI†). Additional control experiments in which Zr^{4+}

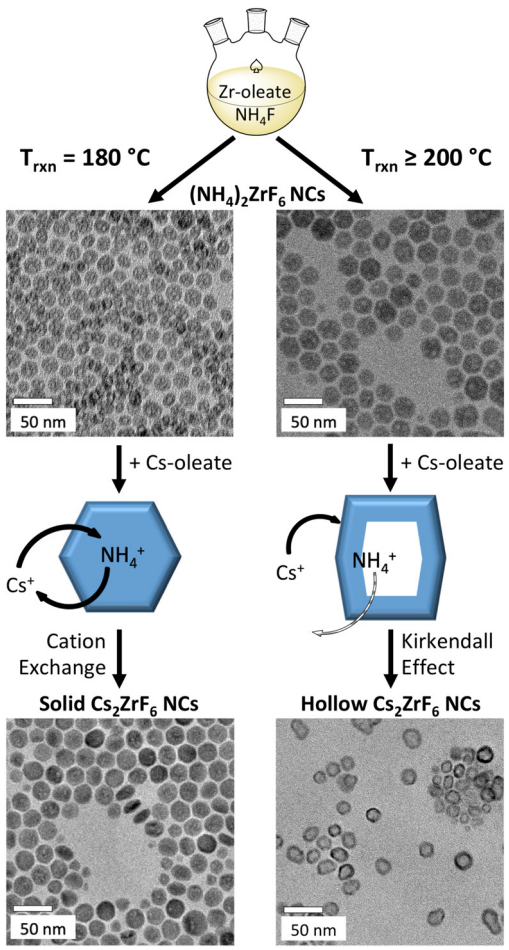

Fig. 4 Mechanisms of Cs_2ZrF_6 NC formation at 180 °C (left) and >200 °C (right). At both temperatures, precursor heating before Cs^+ injection forms similar hexagonal $(NH_4)_2ZrF_6$ NCs. Injection of Cs-oleate at 180 °C yields solid hexagonal Cs_2ZrF_6 NCs *via* balanced A-site cation exchange, but at >200 °C yields hollow Cs_2ZrF_6 NCs *via* a Kirkendall effect caused by imbalanced NH_4^+ and Cs^+ diffusion rates during the cation exchange.

was omitted but other parameters were held constant failed to yield Cs_2ZrF_6, ruling out CsF as a viable intermediate in the direct pathway to the isolated Cs_2ZrF_6 NCs (Fig. S12, ESI†).

In summary, a unique hot-injection synthesis of hexagonal Cs_2ZrF_6 NC colloids that avoids the handling of toxic HF has been developed. The incompatibility between the tetravalent Zr^{4+} and TFA, a common HF alternative in many NC syntheses, led to identification of NH_4F solubilized in MeOH as an attractive and potent fluoride precursor for A_2BF_6 NC syntheses. Analysis of this synthesis revealed formation of hexagonal $(NH_4)_2ZrF_6$ NCs as a reaction intermediate that can be isolated when Cs^+ is omitted entirely. These $(NH_4)_2ZrF_6$ NCs are converted into Cs_2ZrF_6 NCs *via* cation exchange, representing the first A-site cation exchange reported for any A_2BF_6 NCs. Cs_2ZrF_6 NC hollowing was observed at temperatures above 200 °C, attributed to an imbalance in NH_4^+ and Cs^+ diffusion rates under these conditions. Hollowing is suppressed by lowering the temperature to 180 °C, ultimately yielding nearly uniform hexagonal Cs_2ZrF_6 NCs. The identification of NH_4F in MeOH as a relatively safe, versatile, and effective fluoride precursor for A_2BF_6 NC syntheses, and of A-site cation exchange as an effective tool for composition control, is anticipated to enable new chemical approaches to A_2BF_6 NCs with rich compositions and desirable physical properties.

This work was primarily supported by the U.S. National Science Foundation (NSF) through the University of Washington (UW) Molecular Engineering Materials Center, a Materials Research Science and Engineering Center (DMR-1719797). Additional support from the UW Clean Energy Institute (graduate fellowship to E. T.) and the Nicole A. Boand Endowed Chair is gratefully acknowledged. Part of this work was conducted at the Molecular Analysis Facility, a National Nanotechnology Coordinated Infrastructure (NNCI) site at UW supported in part by the NSF (awards NNCI-2025489, NNCI-1542101), the Molecular Engineering & Sciences Institute, and the Clean Energy Institute. The authors thank Thom Snoeren for performing SEM-EDX, Dr. Kyle Kluherz for performing HAADF-STEM, and Kelly Walsh and Prof. Brandi Cossairt for thoughtful discussions.

Conflicts of interest

There are no conflicts to declare.

References

1 M. F. Torresan and A. Wolosiuk, *ACS Appl. Bio Mater.*, 2021, **4**, 1191.
2 E. C. Ximendes, U. Rocha, K. U. Kumar, C. Jacinto and D. Jaque, *Appl. Phys. Lett.*, 2016, **108**, 253103.
3 P. Huang, W. Zheng, S. Zhou, D. Tu, Z. Chen, H. Zhu, R. Li, E. Ma, M. Huang and X. Chen, *Angew. Chem., Int. Ed.*, 2014, **53**, 1252.
4 S. Heer, K. Kömpe, H. U. Güdel and M. Haase, *Adv. Mater.*, 2004, **16**, 2102.
5 C. P. Guntlin, K. V. Kravchyk, R. Erni and M. V. Kovalenko, *Sci. Rep.*, 2019, **9**, 6613.
6 F. Maye and A. Turak, *Radiation*, 2021, **1**, 131.
7 B. Ritter, P. Haida, F. Fink, T. Krahl, K. Gawlitza, K. Rurack, G. Scholz and E. Kemnitz, *Dalton Trans.*, 2017, **46**, 2925.
8 H. Samarehfekri, M. Ranjbar, A. Pardakhty and A. Amanatfard, *J. Cluster Sci.*, 2020, **31**, 453.
9 H. Zhu, C. C. Lin, W. Luo, S. Shu, Z. Liu, Y. Liu, J. Kong, E. Ma, Y. Cao, R.-S. Liu and X. Chen, *Nat. Commun.*, 2014, **5**, 1.
10 D. Chen, Y. Zhou and J. Zhong, *RSC Adv.*, 2016, **6**, 86285.
11 M. Wermuth and H. U. Güdel, *J. Phys.: Condens. Matter*, 2001, **13**, 9583.
12 C. C. Lin, A. Meijerink and R.-S. Liu, *J. Phys. Chem. Lett.*, 2016, **7**, 495.
13 F. Tang, Z. Su, H. Ye, M. Wang, X. Lan, D. L. Phillips, Y. Cao and S. Xu, *J. Mater. Chem. C*, 2016, **4**, 9561.
14 T. A. Cohen, D. Sharp, K. T. Kluherz, Y. Chen, C. Munley, R. T. Anderson, C. J. Swanson, J. J. De Yoreo, C. K. Luscombe, A. Majumdar, D. R. Gamelin and J. D. Mackenzie, *Nano Lett.*, 2022, **22**, 5681.
15 J. Zhu and M. C. Hersam, *Adv. Mater.*, 2017, **29**, 1603895.
16 S. Adachi and T. Takahashi, *J. Appl. Phys.*, 2008, **104**, 023512.
17 A. G. Paulusz, *J. Electrochem. Soc.*, 1973, **120**, 942.
18 Q. Zhou, H. Tan, Y. Zhou, Q. Zhang, Z. Wang, J. Yan and M. Wu, *J. Mater. Chem. C*, 2016, **4**, 7443.
19 L. Huang, Y. Zhu, X. Zhang, R. Zou, F. Pan, J. Wang and M. Wu, *Chem. Mater.*, 2016, **28**, 1495.
20 X. Luo, Z. Hou, T. Zhou and R. J. Xie, *J. Am. Ceram. Soc.*, 2020, **103**, 1018.
21 K. E. Yorov, W. J. Mir, X. Song, L. Gutiérrez-Arzaluz, R. Naphade, S. Nematulloev, C. Chen, R.-W. Huang, B. Shao, B. E. Hasanov, Y. Han, O. F. Mohammed and O. M. Bakr, *ACS Mater. Lett.*, 2022, **4**, 2273.
22 R. G. Szlag, L. Suescun, B. D. Dhanapala and F. A. Rabuffetti, *Inorg. Chem.*, 2019, **58**, 3041.
23 H. N. Munasinghe, L. Suescun, B. D. Dhanapala and F. A. Rabuffetti, *Inorg. Chem.*, 2020, **59**, 17268.
24 J. C. Boyer, L. A. Cuccia and J. A. Capobianco, *Nano Lett.*, 2007, **7**, 847.
25 M. Wörle, C. P. Guntlin, L. Gyr, M. T. Sougrati, C.-H. Lambert, K. V. Kravchyk, R. Zenobi and M. V. Kovalenko, *Chem. Mater.*, 2020, **32**, 2482.
26 C. Rüssel, *J. Non-Cryst. Solids*, 1993, **152**, 161.
27 M. J. Baillie, D. H. Brown, K. C. Moss and D. W. A. Sharp, *J. Chem. Soc. A*, 1968, 3110.
28 J. Farjas, J. Camps, P. Roura, S. Ricart, T. Puig and X. Obradors, *Thermochim. Acta*, 2012, **544**, 77.
29 H. N. Munasinghe, M. R. Imer, R. G. Szlag, L. Seuscun and F. A. Rabuffetti, *Dalton Trans.*, 2022, **51**, 18224.
30 S. D. Schimler, S. J. Ryan, D. C. Bland, J. E. Anderson and M. S. Sanford, *J. Org. Chem.*, 2015, **80**, 12137.
31 V. Iashin, T. Wirtanen and J. E. Perea-Buceta, *Catalysts*, 2022, **12**, 233.
32 F. Wang, R. Deng and X. Liu, *Nat. Protoc.*, 2014, **9**, 1634.
33 Z. Li and Y. Zhang, *Nanotechnology*, 2008, **19**, 345606.
34 J. Song, G. Wang, S. Ye, Y. Tian, M. Xiong, D. Wang, H. Niu and J. Qu, *J. Alloys Compd.*, 2016, **658**, 914.
35 L. K. Bharat, G. Nagaraju, G. S. R. Raju, Y.-K. Han and J. S. Yu, *Part. Part. Syst. Charact.*, 2018, **35**, 1800018.
36 F. Zhang, Y. Shi, X. Sun, D. Zhao and G. D. Stucky, *Chem. Mater.*, 2009, **21**, 5237.
37 L. Li, Y. Tang, Y. Zhang, J. Yang and B. Du, *Front. Chem.*, 2008, **3**, 76.
38 Y. Yin, R. M. Rioux, C. K. Erdonmez, S. Hughes, G. A. Somorjai and A. P. Alivisatos, *Science*, 2004, **304**, 711.

